U.S. DEPARTMENT OF ENERGY | Office of Science

DOE/SC-ARM-TR-320

Fixed-Site KAZR b1 Data Processing: Corrections, Calibrations, and Processing Report

M Rocque
E Schuman
A Matthews
Y-C Feng
M Deng
T Wendler

September 2025

ARM

DISCLAIMER

DOE/SC-ARM-TR-320

Fixed-Site KAZR b1 Data Processing: Corrections, Calibrations, and Processing Report

M Rocque, Pacific Northwest National Laboratory (PNNL)
Y-C Feng, PNNL
E Schuman, PNNL
M Deng, Brookhaven National Laboratory
A Matthews, PNNL
T Wendler, PNNL

September 2025

How to cite this document:

Rocque, M, Y-C Feng, E Schuman, M Deng, A Matthews, and T Wendler. Fixed-Site KAZR b1 Data Processing: Corrections, Calibrations and Processing Report. U.S. Department of Energy, Atmospheric Radiation Measurement user facility, Richland, Washington. DOE/SC-ARM-TR-320.

Work supported by the U.S. Department of Energy,
Office of Science, Office of Biological and Environmental Research

Acronyms and Abbreviations

2D	two-dimensional
AFB	air force base
ARM	Atmospheric Radiation Measurement
ARSCL	Active Remote Sensing of Clouds Value-Added Product
CPR	cloud profiling radar
DOE	U.S. Department of Energy
EIKA	extended interaction Klystron amplifier
ENA	Eastern North Atlantic
GE	general mode
KAZR	Ka-band ARM Zenith Radar
KAZR2	second-generation Ka-band ARM Zenith Radar
KAZRCOR	KAZR Corrected Data Value-Added Product
LD	laser disdrometer
LDQUANTS	Laser Disdrometer Quantities Value-Added Product
LPM	laser precipitation monitor
MCC	mission control computer
MD	moderate mode
MOSAiC	Multidisciplinary Drifting Observatory for the Study of Arctic Climate
NEXRAD	Next-Generation Weather Radar
NSA	North Slope of Alaska
PNNL	Pacific Northwest National Laboratory
PPI	plan position indicator
PR	precipitation mode
Py-ART	Python ARM Radar Toolkit
RDS	radar data system
RF	radio frequency
RWP	radar wind profiler
SACR2	second-generation Scanning ARM Cloud Radar
SGP	Southern Great Plains
SNR	signal-to-noise ratio
TWTA	traveling-wave tube amplifier
UTC	Coordinated Universal Time
VD	video disdrometer
VDISQUANTS	Video Disdrometer Value-Added Product
XSAPR2	second-generation X-band Scanning ARM Precipitation Radar
ZDR	differential reflectivity

Contents

Figures

Tables

1.0 Introduction

The U.S. Department of Energy's (DOE) Atmospheric Radiation Measurement (ARM) User Facility operates three fixed-site observatories: Eastern North Atlantic (ENA), North Slope of Alaska (NSA), and Southern Great Plains (SGP). Each fixed site has a wide variety of atmospheric instrumentation that has been collecting data for at least 10 years (NSA and SGP over 25 years). Each site is unique because it represents a different climate state. The environment at ENA is characterized by marine stratocumulus clouds and one of the key scientific areas of focus is the interaction of these clouds with aerosols. At NSA the focus is on arctic climate and cloud and radiative processes in a high-latitude environment. SGP represents a mid-latitude, mid-continent climate that experiences environmental cycles on diurnal and seasonal time scales. The ARM observatories are all meant to improve understanding of atmospheric processes that can then be better incorporated into weather and climate models. Another common thread between the fixed sites is the focus on cloud processes. Each site is equipped with at least one radar that provides continuous remote-sensing observations of clouds and precipitation.

This report details the analysis of a1-level radar data at the fixed sites and the process for generating b1-level data. While b1-level data have been produced for ARM campaigns at the mobile facilities, this is the first analysis led by ARM radar mentors to correct data at the fixed sites. In particular, we focus on calibrations and corrections of the Ka-band ARM Zenith Radars (KAZRs) at ENA, NSA, and SGP. Ongoing and future work will involve corrections applied to other fixed-site radars.

1.1 Overview of Fixed-Site KAZRs

Each of the ARM observatories has a KAZR collocated with other instruments and radars (Figure 1). At ENA, the KAZR is second generation (KAZR2) and is located near the second-generation Scanning ARM Cloud Radar (SACR2; W-band and Ka-band), and the second-generation X-band Scanning ARM Precipitation Radar (XSAPR2). There are also disdrometers and a 1290 MHz radar wind profiler (RWP) at the site. At NSA, the KAZR is collocated with the SACR2 (W-band and Ka-band) and is about 2.1 km east of the XSAPR. In addition to the radars, there is a laser precipitation monitor (LPM) at the central facility. At SGP, the KAZR is collocated with the 915 MHz RWP and disdrometers. There is an XSAPR about 19 km northwest of the central facility, and the WSR-88D KVNX (Vance Air Force Base (AFB), Oklahoma) is about 60 km west of the KAZR. While the KAZRs and disdrometers are continuously operating, other radars at and around the sites are not necessarily operational during the calibration period (January 2020-December 2024).

The KAZR specifications including frequency, polarization, gate resolution, minimum and maximum range, and mode of operation (among other parameters) are listed in Table 1. Each KAZR has some similarities and some differences. The biggest differences typically arise between the KAZR and KAZR2. The KAZR2 has a different transmitter (extended interaction Klystron amplifier (EIKA) instead of a traveling-wave tube amplifier or TWTA) that results in higher transmit power and greater sensitivity. The KAZR2 also operates with three modes instead of two. The three KAZR modes are general (GE), moderate (MD), and precipitation (PR) sensitivity. The GE and PR modes emit simple burst pulses while the MD mode pulse is longer and frequency modulated, resulting in higher sensitivity but a larger blind zone near the radar. Thus, the GE mode is typically used for comparisons and analyses close to the radar

(within the lowest 1 km or so) while the MD mode is best used throughout the rest of the column. The PR mode is only available for the KAZR2 and is meant to be used in heavy rain close to the radar.

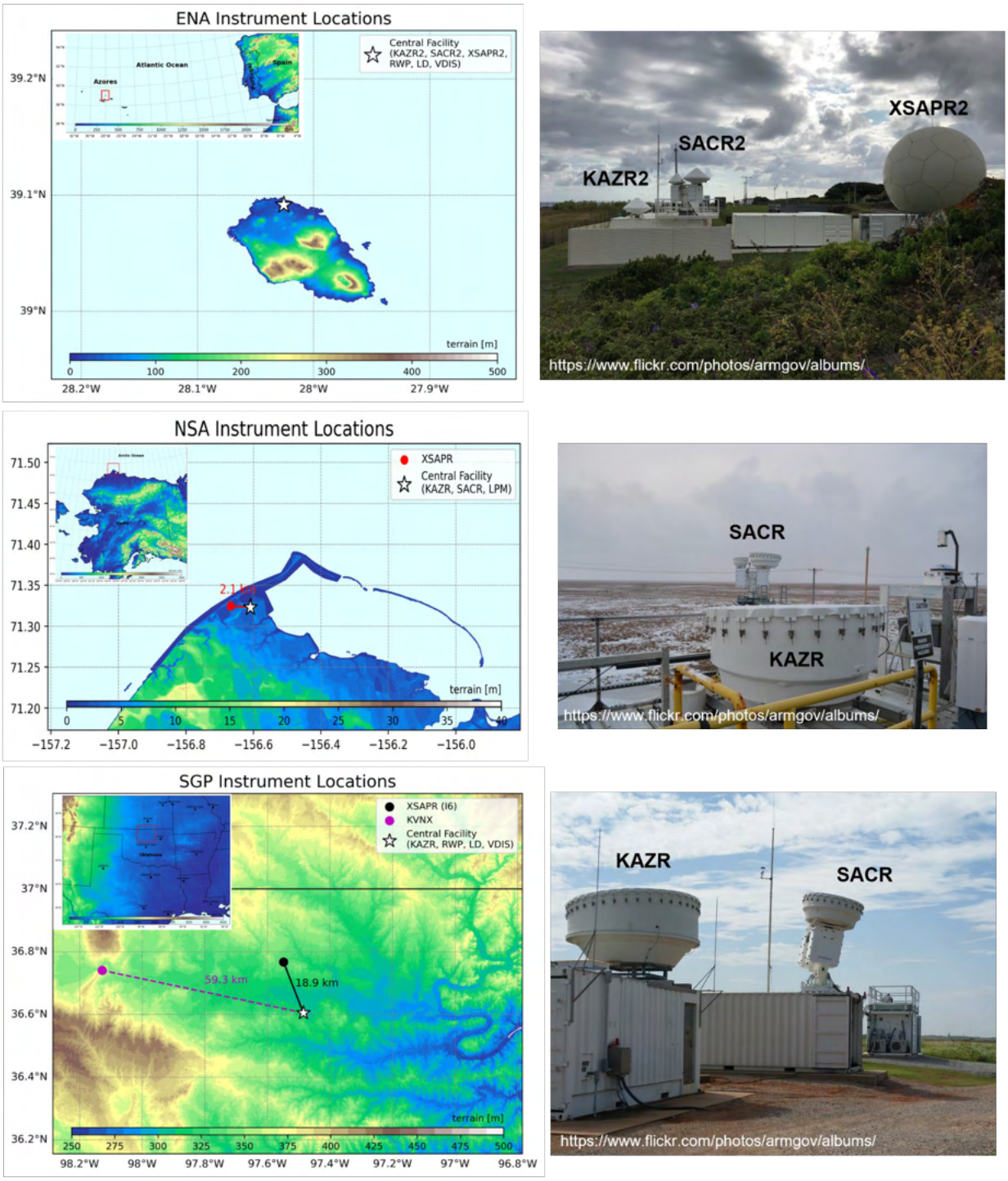

Figure 1. Left: Map of ARM fixed sites (top: ENA, middle: NSA, bottom: SGP) with terrain heights (m) shaded. Each map has an insert in the top left with a zoomed-out map of the area for context. Right: ARM radars installed at each fixed site. Images are taken from the ARM flickr page: https://www.flickr.com/photos/armgov/albums/.

Table 1. Specifications of each KAZR/KAZR2 at ENA, NSA, and SGP.

	ENA	NSA	SGP
Frequency (GHz)	34.8	34.9	34.9
Wavelength (mm)	8.61	8.59	8.59
Transmitter type	EIKA	TWTA	TWTA
Transmit power (kW)	2.0 kW	0.2	0.2
Transmit polarization	dual	single	single
Receive polarization	dual	dual	dual
Antenna diameter (m)	1.8	2.0	3.0
3 dB beam width (deg)	0.3	0.3	0.2
Gate spacing (m)	29.98	29.98	29.98
Nyquist velocity (m s^{-1})	5.98	5.96	5.96
Operating mode	GE, MD, PR	GE, MD	GE, MD
Minimum range (m; GE/MD/PR)	72/708/72	101/868	101/568
Maximum range (km)	18.2	17.5	20.4
Far-field range (m)	761	931	2095
Temporal resolution (s)	2.0	3.7	3.9

1.2 Radar Performance

Figure 2 shows the percentage of data files available for each KAZR compared to the maximum files available per day (24). The KAZRs have been consistently running for nearly the entire period from January 2020 through December 2024. At ENA, there was a period of missing data in May-June 2020 that can be attributed to a hardware issue. At SGP, two gaps in data are visible: one in September-October 2020 when the transmitter was not working properly and the other in April-May 2023 due to a problem with the air conditioning system.

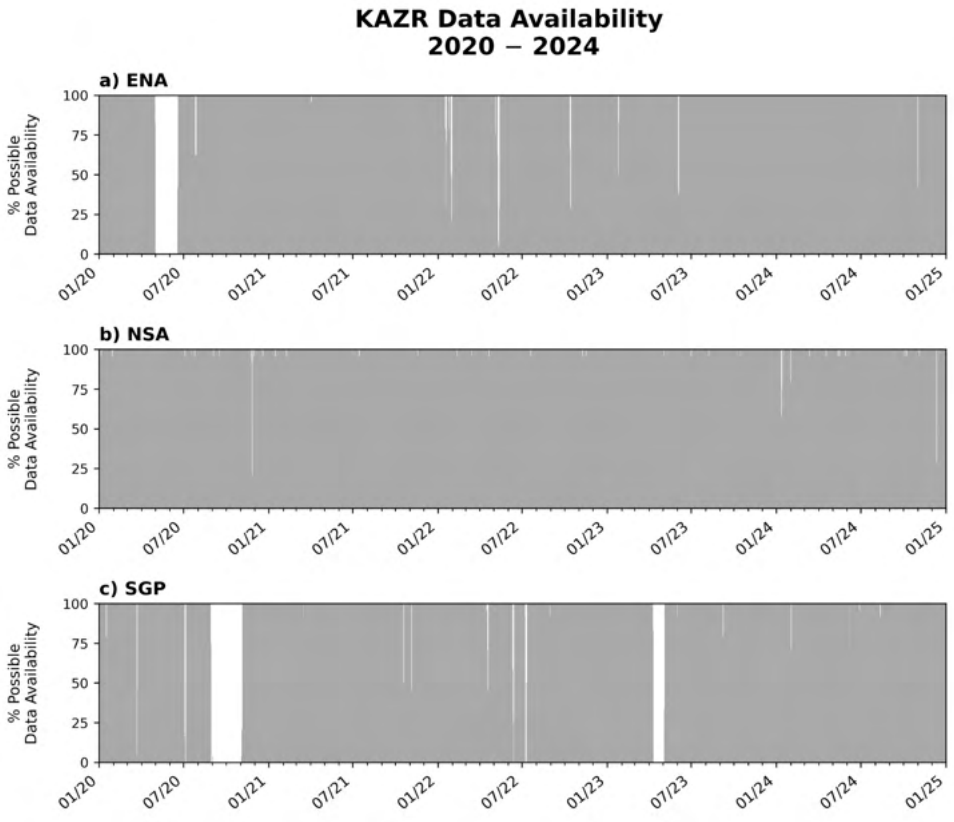

Figure 2. KAZR data availability at a) ENA, b) NSA, and c) SGP for 2020 through 2024.

The KAZR hardware parameters were also assessed to determine if there were any major changes over the five-year period. Figure 3 shows time series plots of the co-polar radar constant for each mode of KAZR at each fixed site. The KAZRs are designed to automatically update the radar constants based on other parameters including the transmit power and the gain. At ENA, the GE and MD radar constants have been increasing over the past five years while the PR mode has been relatively consistent. At NSA, the radar constants do not automatically update until October 2021 when a significant jump of 2-4 dB is observed. The radar constants remain relatively flat the remainder of the period until July 2024 when the GE-mode constant decreases about 1 dB associated with work performed by the radar engineer. At SGP, the radar constants were not automatically updated until August 2023 but similarly remain relatively constant afterwards. Radar sky noise and transmit power were also analyzed and no significant trends or changes were observed for NSA and SGP (not shown). However, the ENA KAZR2 transmit power has been declining over the past five years, which explains the increasing trend in the radar constant.

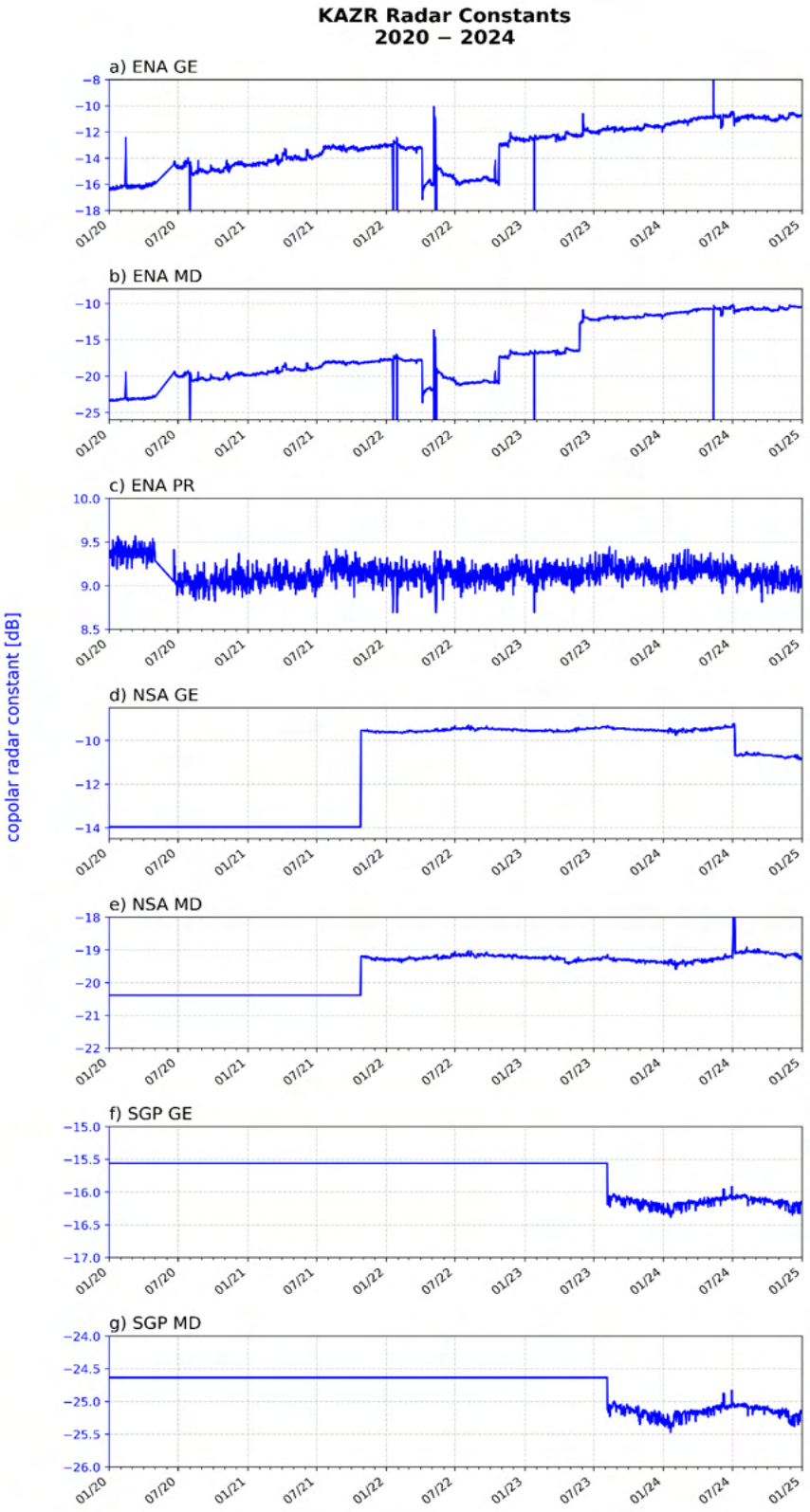

Figure 3. Time series of co-polar radar constants for each KAZR mode at each fixed site from 2020 through 2024: a) ENA GE, b) ENA MD, c) ENA PR, d) NSA GE, e) NSA MD, f) SGP GE, and g) SGP MD.

1.3 Outline for b1 Processing

The two main tasks for processing a-level KAZR data into b-level data involve applying offsets to the reflectivity field and creating an echo mask that can be used to remove any non-meteorological signals. The calibration of reflectivity for KAZR in particular is more limited compared to calibration of scanning radars due to the vertically pointing nature of the radar. Thus, KAZR reflectivity calibration relies on intercomparisons with other instruments, most often disdrometers and other nearby radars. Results of these comparisons applied to each fixed site are detailed in Section 2.

Like other radars, the KAZR measures backscatter from a number of different signals, some of which are non-meteorological in nature. The b-level data contains an additional mask that identifies non-meteorological signals and categorizes them into background noise, clutter, biota, or range sidelobes. This mask can be used by scientists to easily filter out the cloud and precipitation data. Examples of the mask applied to the fixed-site KAZRs are shown in Section 3.

2.0 Calibrations and Corrections

Traditional calibration techniques that are applied to scanning radars such as solar calibration, use of a corner reflector, or relative calibration adjustment that monitors the ground clutter stability cannot be performed on zenith-pointing radars. The following subsections describe various methodologies for KAZR reflectivity calibration; Section 2.5 provides a summary of the final offsets for each site.

2.1 Gas Attenuation

Depending on the local environment, attenuation due to atmospheric water vapor can lead to a significant decrease in the power returned to the radar at millimeter wavelengths. Examples of how the gas attenuation varies in different environments is shown in Figure 4. For a moist profile at ENA, the two-way gas attenuation for KAZR can be close to 1.4 dB. Meanwhile at NSA, despite the profile being saturated at several heights, the amount of water vapor is low, resulting in little attenuation. A mixed profile at SGP with a large dry air level between 500 and 300 hPa has higher gas attenuation than NSA, with two-way attenuation up to 0.8 dB. While the gas attenuation correction is not included in the b1-level data, it is considered for all analyses when determining the KAZR reflectivity offsets. The gas attenuation is included in the c-level KAZR Corrected Data (KAZRCOR) Value-Added Product (VAP) and the Active Remote Sensing of Clouds (ARSCL) VAP.

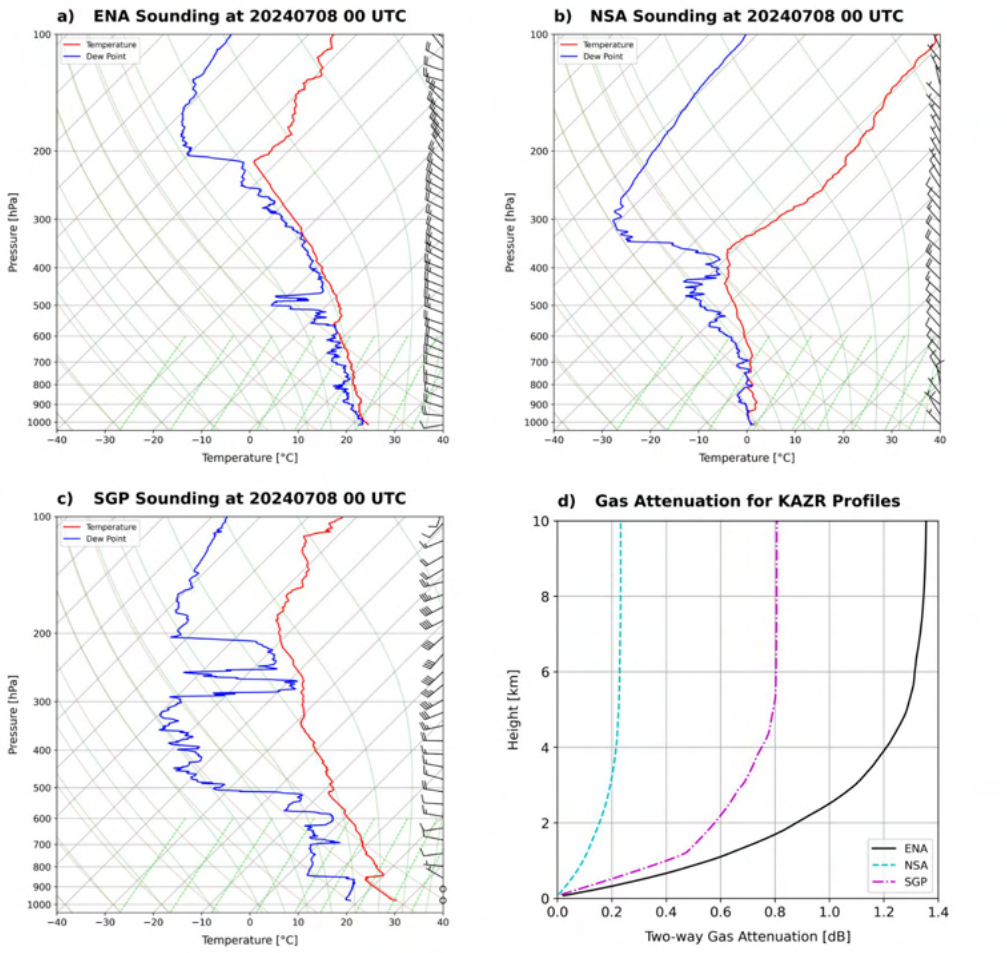

Figure 4. Skew-T log-p diagrams from 8 July 2024 00 UTC soundings at a) ENA, b) NSA, and c) SGP. Red (blue) lines are the temperature (dew point) (°C) and the wind barbs are plotted on the right axes (m s^{-1}). d) Profiles of the two-way cumulative gas attenuation (dB) for the KAZR at each site (ENA solid black; NSA dashed cyan; SGP dot-dashed magenta).

2.2 KAZR Intermodal Comparison

At each site, the GE and MD modes are compared to each other to determine any initial reflectivity offsets. The GE and MD files are first interpolated to the same range. Matching gates are then compared if the signal-to-noise ratio (SNR) is greater than 0 dB and the reflectivity is between -5 and 15 dBZ. The points are then averaged by day and daily mean differences between GE and MD mode are plotted (Figure 5). These days have at least 1000 points and the standard deviation of the difference is less than 1.5 dB.

At ENA, there are three distinct periods in which the differences are stable in time. The first is from 1 January 2020 through 2 May 2020 where the GE mode is about 0.7 dB higher than the MD mode. After the oscillator was replaced, the GE mode is about 0.3 dB less than the MD mode until 25 May 2023. On 25 May 2023, the MD filter was changed, resulting in the MD mode being about 2.5 dB higher than the GE mode.

As NSA, the GE mode is about 2.2 dB lower than the MD mode until 26 October 2021 when the radar constants are updated. Afterwards, the GE mode is about 0.9 dB higher than MD until 8 May 2024 when the difference drops to -1.8 dB. This decrease in May appears to be related to issues with the radar mission control computer (MCC) and the radar data system (RDS). The GE cross-polar reflectivity also experienced a significant jump during this period, increasing about 12 dB higher than the MD cross-polar reflectivity (not shown). When comparing May and June data from 2023 and 2024 for both GE and MD modes, there is a shift in the GE mean reflectivity between the two years that is not seen in the MD mode (not shown). This confirms that the difference is due to changes in the GE mode. A radar reset was performed by the engineer on 1 July 2024 that returned the reflectivity difference between the two modes to 0.9 dB. Additional work was performed by the engineer on 3 December 2024 that decreased the difference between the two modes to about 0.3 dB.

At SGP, the offset between the modes is about 0.5 dB until the radar stopped transmitting in July 2020. After the radio frequency (RF) unit and transmitter were repaired, the offset between modes is fairly stable with the GE mode about 0.3 dB higher than the MD mode. Standard deviations at each site are around 1 dB.

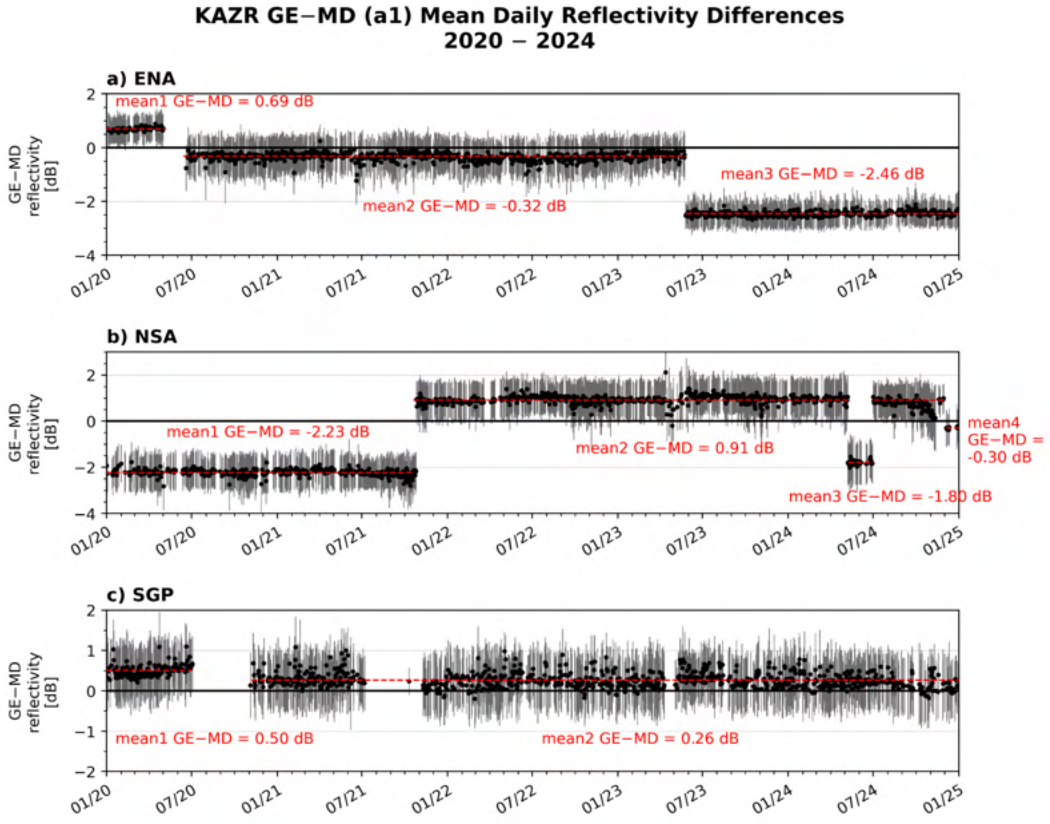

Figure 5. Time series of daily mean differences between KAZR a1 GE- and MD-mode reflectivity at a) ENA, b) NSA, and c) SGP for 2020 through 2024. The means are shown in the red dashed lines and averages across each period are included on each subplot.

The ENA KAZR2 has an additional mode (PR) that can be compared with the GE mode. As shown in Figure 3, the PR-mode calibration constant is not updated to reflect the declining transmit power. Before comparisons between modes can be made, we first calculate the correction due to the declining power

based on the initial transmit power on 1 January 2020. Over the five-year period, the transmit power drops about 6 dBm, which corresponds to about a 6 dB increase in reflectivity (Figure 6). Four periods are detected where the EIKA correction slope is around 0.003 dB day^{-1} but with varying initial offsets. These time periods are outlined in Table 2. The PR-mode reflectivity is corrected for the decline with these four equations and comparisons are run for GE and PR mode. Figure 7 shows the difference between the two modes with another four distinct periods where the offset changes. Notably, correcting for the EIKA power decline results in relatively consistent trends within the four periods. The offsets vary between 7 and 10.5 dB, suggesting the PR mode is significantly lower than the GE mode. An example case from ENA on 16 October 2022 is shown to highlight the sensitivity differences between the GE, MD, and PR modes (Figure 8).

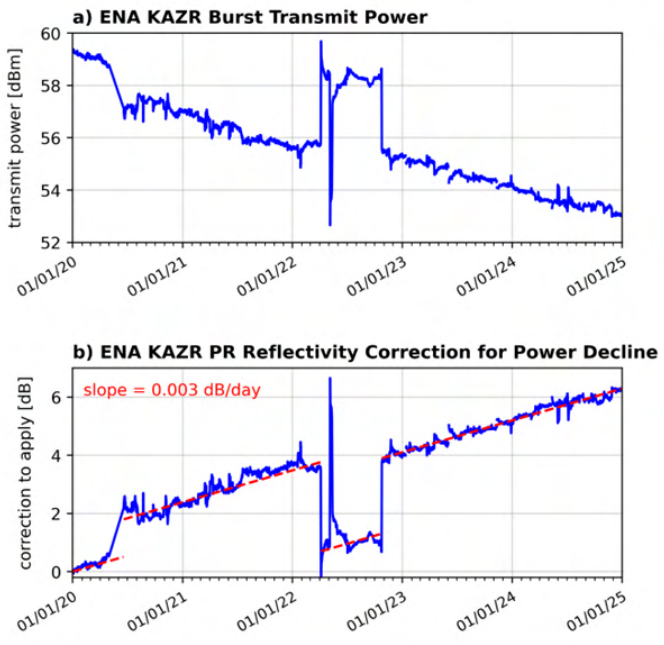

Figure 6. Time series of ENA KAZR a) burst-mode transmit power (dBm) and b) reflectivity offset applied to the PR mode to correct for the transmit power decline (dB) for 2020 through 2024. The red dashed lines in panel b) show the lines of best fit for each time period.

Table 2. Time periods and corresponding linear trends applied to correct for the ENA KAZR2 transmit power decline.

Time period	Linear trend for EIKA correction
20200101-20200618	0.003t + 0.0 dB (t = *days since 20200101*)
20200618-20220406	0.003t + 1.8 dB (t = *days since 20200618*)
20220406-20221025	0.003t + 0.7 dB (t = *days since 20220406*)
20221025-20250101	0.003t + 3.9 dB (t = *days since 20221025*)

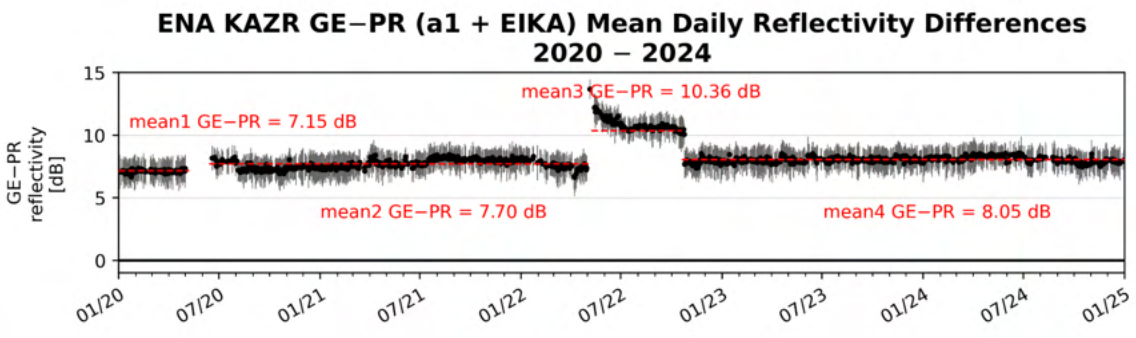

Figure 7. Time series of daily mean differences between ENA KAZR2 GE- and PR-mode reflectivity for 2020 through 2024 after corrections for declining power. There are four offset periods, and the mean offset for each period is shown in the red dashed lines and varies between 7 and 10.5 dB.

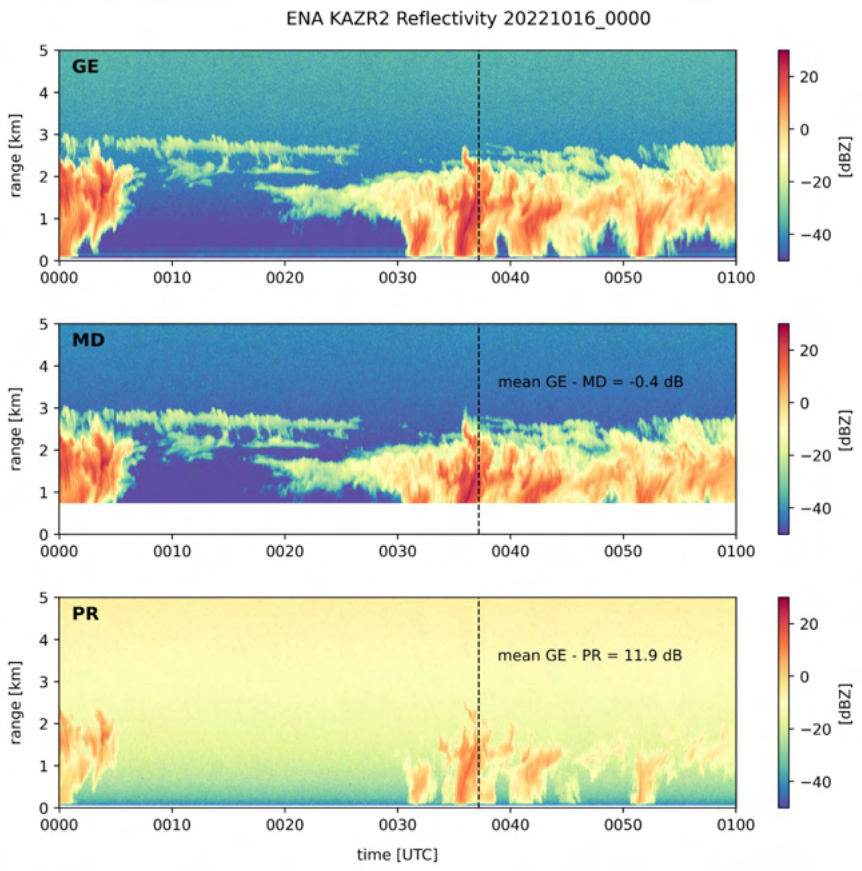

Figure 8. Time-height plots of reflectivity (dBZ) from the ENA KAZR2 GE (top), MD (middle), and PR (bottom) modes on 16 October 2022 from 00-01 UTC. Differences between the modes are calculated at the dashed line and are included on the MD- and PR-mode plots (GE - MD = -0.4 dB, GE - PR = 11.9 dB).

2.3 KAZR Cross-Comparisons with Disdrometers

Each ARM observatory has at least one disdrometer collocated with the KAZR. For this analysis, we assume the disdrometer is "truth" and calibrate the KAZRs based on this data. At ENA and SGP, there is a laser disdrometer (LD) and a video disdrometer (VDIS). Both of these disdrometers have associated VAPs that calculate advanced parameters including frequency-specific reflectivity (Laser Disdrometer Quantities Value-Added Product [LDQUANTS], Video Disdrometer Value-Added Product [VDISQUANTS]; Hardin et al. 2020). In this analysis, the Ka-band reflectivity from the disdrometer VAP is compared with KAZR GE-mode reflectivity at 500 m above ground level at ENA and SGP. KAZR profiles within two minutes of the nearest disdrometer sample are averaged to account for differences between 500 m and the surface potentially due to advection/shear, evaporation, or sorting. The KAZR profiles are corrected for gas attenuation following Ulaby et al. (198)1 and a near-field correction is added (Sekelsky 2001; ENA = 0.1 dB, NSA = 0.2 dB, SGP = 1.5 dB). Different thresholds on reflectivity values are then applied to each site to best ensure the comparisons will result in the system calibration offset. The thresholds are meant to reduce or eliminate other potential factors impacting the reflectivity bias such as hydrometeor or wet radome attenuation, Mie scattering, or impacts from non-meteorological targets.

A similar method is applied at NSA. However, there is only a laser precipitation monitor (LPM) on site that does not currently have any advanced products associated with it. The LPM software does calculate reflectivity, but it assumes S-band frequency and there are no additional checks on reflectivity accuracy. A separate analysis of S-band versus Ka-band reflectivity from the disdrometer VAPs at different sites showed that there are very small differences between the two frequencies at the lower reflectivity values that are being applied here (< 15 dBZ), so the S-band assumption should not lead to any significant biases. Since the disdrometer comparison is only valid for liquid particles, the analysis at NSA is limited to a few months each summer. As with ENA and SGP, several thresholds are applied to ultimately estimate the KAZR calibration offset. Results from each analysis at each site are presented below.

2.3.1 ENA KAZR versus LD

In addition to the KAZR GE and LD reflectivity, several other parameters from different instruments are analyzed to determine the optimal conditions to perform the comparisons. Figure 9 shows two-dimensional (2D) histograms of the reflectivity difference between KAZR GE and LD versus variables such as linear depolarization ratio (LDR) from the KAZR, surface temperature, relative humidity, winds, and rain rate. There tends to be larger differences at higher LDR values (> -20 dB), at higher relative humidity (> 90%), and at higher rain rates (> 0.3 mm hr^{-1}). There are no clear correlations between the reflectivity difference and the temperature or winds, although temperatures are typically above 10°C and the predominant wind direction is from the southwest.

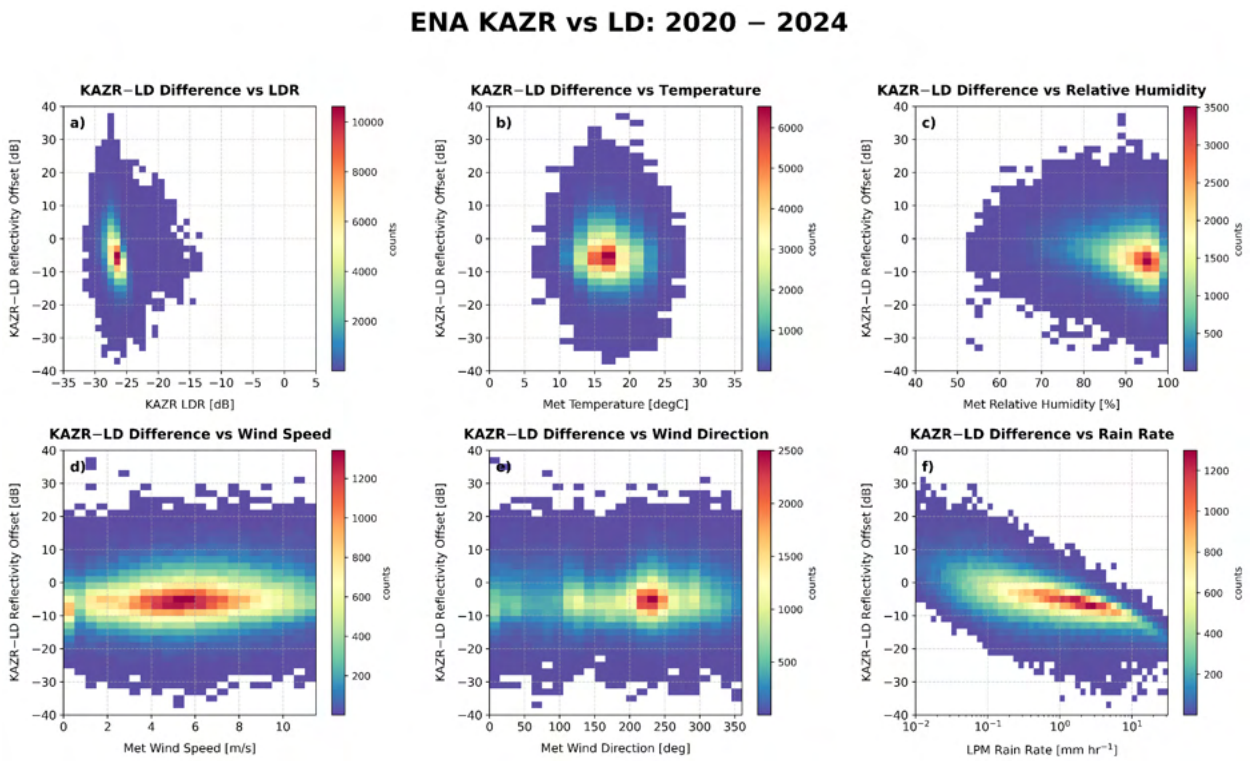

Figure 9. 2D histograms of ENA KAZR GE-LD reflectivity versus a) KAZR LDR (dB), b) 2-meter temperature (°C), c) 2-meter relative humidity (%), d) 10-meter wind speed (m s^{-1}), e) 10-meter wind direction (°), and f) rain rate from the LD (mm hr^{-1}). Colors represent the number of samples within each 2D bin from January 2020 through December 2024.

Once thresholds are applied to the data set, the KAZR GE reflectivity can be directly compared with the LD reflectivity. Histograms of KAZR and LD reflectivity are shown in Figure 10. The distributions align well with mean KAZR and LD reflectivity within 0.2 dB of each other. KAZR versus LD reflectivity shown in the 2D histogram generally follows the one-to-one line and there is a maximum in points around 5-15 dBZ (Figure 10b). The mean offset between KAZR GE and LD is 0.1 dB when considering all reflectivity points. To further reduce the impacts of hydrometeor attenuation, we can filter the points with reflectivity between -5 and 15 dBZ. This results in an average offset of around -0.5 dB.

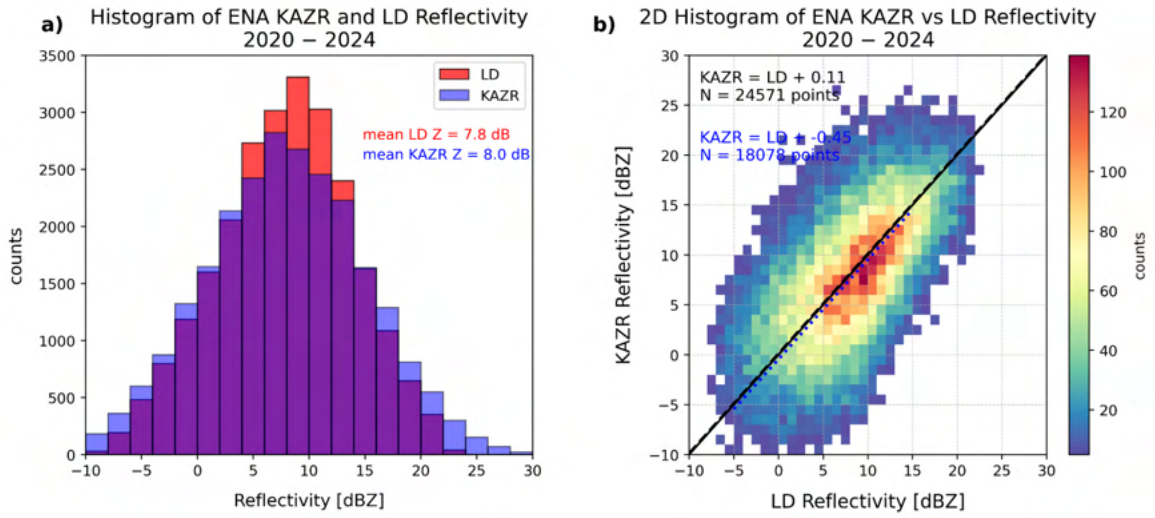

Figure 10. a) Histogram of Ka-band reflectivity from the ENA LDQUANTS VAP (red) and the ENA KAZR GE mode (blue). The mean is shown in the upper left (7.8 dBZ for LD, 8.0 dBZ for KAZR). b) 2D histogram of ENA KAZR a1 GE-mode reflectivity versus Ka-band LD reflectivity with colors corresponding to the number of points within each bin. A one-to-one line is shown in solid black, a fitted line for all data points is shown in dashed black, and a fitted line for reflectivity between -5 and 15 dBZ is shown in dotted blue. The offsets for the fitted lines are shown in the upper left along with the total number of points. The mean offset between KAZR and LD is -0.5 dB when points are between -5 and 15 dBZ. The correlation between KAZR and LD reflectivity is 0.57.

The points can then be grouped by day to evaluate how stable the offset is over time. Figure 11 shows a time series of the daily mean differences between KAZR GE and LD reflectivity where the daily standard deviation is less than 5 dB and the number of daily comparison points is greater than 10. While there is some variability across the time frame, the trend appears to be relatively flat until late 2023 when the difference begins to increase. This trend is likely due to an issue with the LD where condensation frequently occurred on the lenses (ARM Data Quality Report D250207.5). Histograms for 2023 and 2024 data split by year also show this shift in the LD reflectivity in 2024 (not shown). Furthermore, the same analysis was completed with the VDIS, which produced consistent results in 2023 and 2024, suggesting the KAZR data quality was consistent (not shown). In summary, the average offset from both the histogram analysis and time series show the KAZR GE mode is well calibrated with a consistent offset of about 0.5 dB over the past five years.

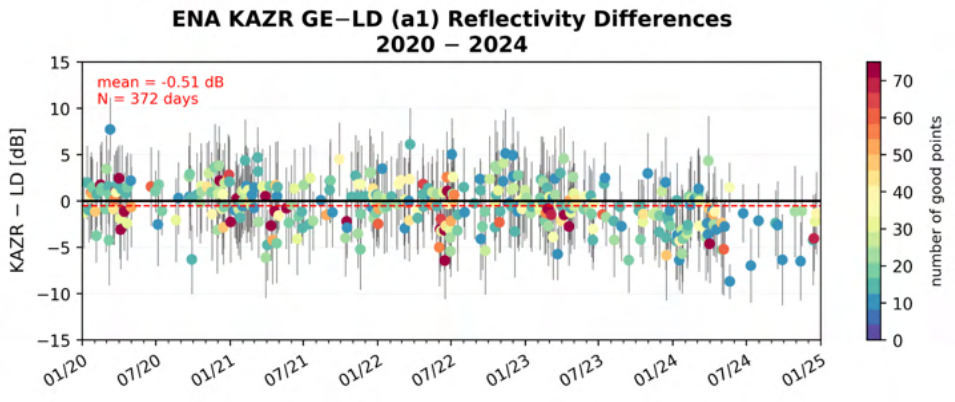

Figure 11. Time series of the daily mean differences between ENA KAZR a1 GE and LD reflectivity (dB). Each point is colored by the number of good points, and the error bars represent the standard deviation for that day. The mean of the daily mean differences is shown in the upper left (-0.5 dB), and is plotted as the red dashed line. 372 days of data were used.

2.3.2 NSA KAZR versus LPM

Conditions at NSA are significantly different than those at ENA. At NSA, a small subset of the data experiences temperatures above 0°C in the summer months. As with ENA, the reflectivity difference between KAZR and the disdrometer (LPM) can be compared with other variables to determine any necessary thresholds (Figure 12). Similarly to ENA, there is not much variability at different temperatures and winds. However, the rain rate at NSA is much lower than ENA and there is a slight increase in reflectivity difference with increasing rain rate.

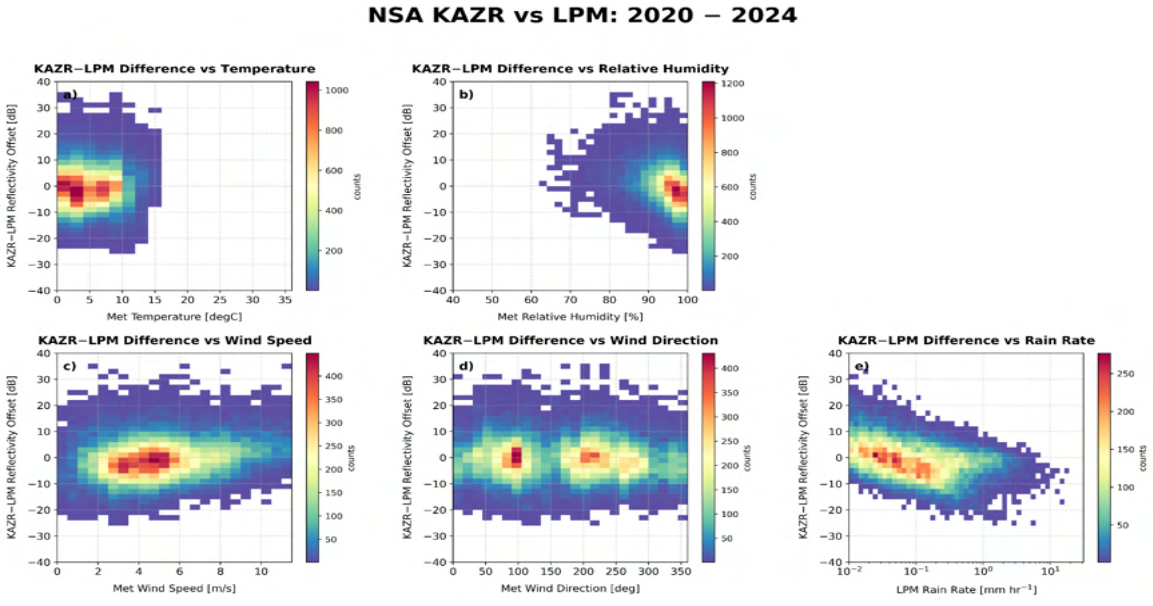

Figure 12. As in Figure 9 but for the NSA KAZR GE mode and the LPM.

As with ENA, thresholds are applied to the data and comparisons between KAZR GE reflectivity and disdrometer reflectivity are made. One caveat with the LPM is it does not have an associated VAP with

calculated radar measurements. However, the instrument does have software that calculates S-band reflectivity that we use for this analysis. Histograms of reflectivity show the KAZR is shifted about 1.2 dB lower than the LPM on average, and most samples occur within -5 to 5 dBZ (Figure 13).

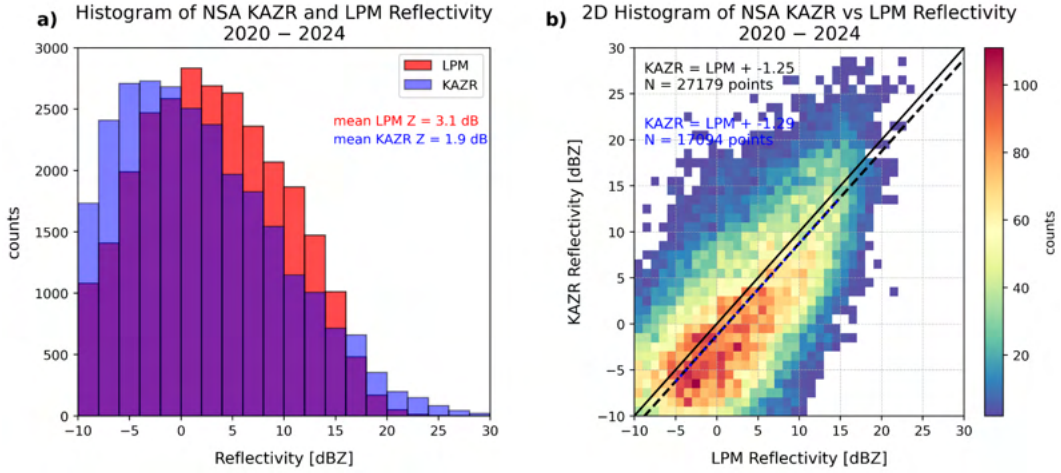

Figure 13. As in Figure 10 but for the NSA KAZR GE mode and the LPM. The mean offset between KAZR and LPM when points are between -5 and 15 dBZ is -1.3 dB. The correlation between KAZR and LPM reflectivity is 0.64.

Time series of daily mean differences between KAZR GE mode and the LPM at NSA are shown in Figure 14 for summer months when the precipitation phase is liquid. The average daily mean offset between KAZR and the LPM is much larger in 2021 at around -4.2 dB compared to subsequent years when the average offset is -0.5 dB. As shown in Figure 3, there was a 4.4 dB shift in the GE radar constant between 2021 and 2022. After the update to the radar constant, the KAZR is in better agreement with the LPM. Histograms split by each year similarly show smaller offsets in 2022-2024 compared to 2021 (not shown). While the KAZR was also operating in 2020, the LPM was removed for repairs so there are very few comparison points. Based on previous studies of NSA KAZR calibration and the consistent radar constant before 2021, we apply a similar 4.1 dB offset to the 2020 KAZR GE data.

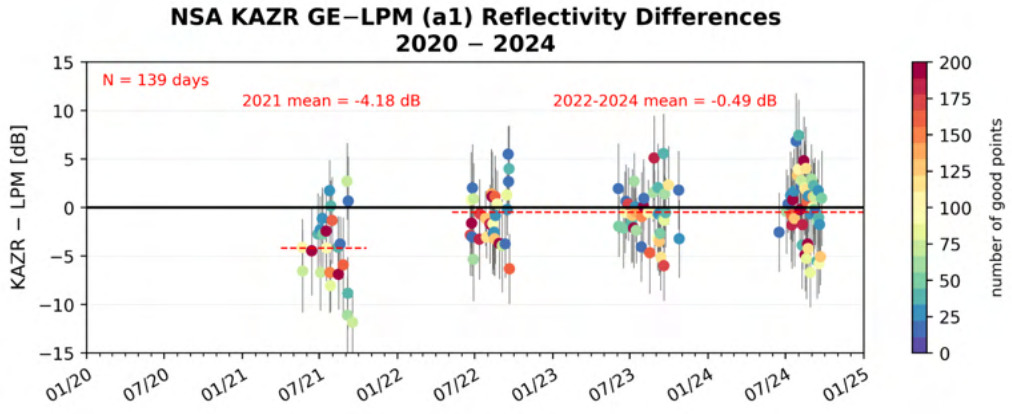

Figure 14. As in Figure 11 but for the NSA KAZR and the LPM. Only times when liquid precipitation was detected are plotted. The mean of the daily mean differences is about -4.2 dB in 2021 and -0.5 dB in 2022 through 2024. 139 days of data were used.

2.3.3 SGP KAZR versus VDIS

The same method applied at ENA is also applied for the SGP KAZR. Here we use the VDIS instead of the LD because the LD had data quality issues in 2021 and 2022 (ARM Data Quality Report D220425.5). Results from the threshold analysis show large biases between KAZR and the VDIS across most parameters (Figure 15). In particular, there is a strong relationship between reflectivity bias and rain rate, and even at smaller rain rates (< 0.1 mm hr-1) the offset is high. Even with thresholds applied to remove higher rain rates and higher relative humidity, histograms of reflectivity also show some bias, with mean KAZR GE reflectivity about 1.6 dB lower than the mean VDIS reflectivity (Figure 16). There is considerably more variability in the 2D histogram analysis compared to ENA and NSA where data tend to follow the one-to-one line more closely (the correlation here is only 0.37). While not shown, the daily mean offsets are also quite variable across the five-year period with the majority of cases showing the KAZR reflectivity at least 5 dB lower than the VDIS. Compared to other sites, there are also significantly fewer comparison points over the past five years.

We suspect the large bias between the KAZR and disdrometer is related to the intense and more convective nature of events observed at SGP. Unlike at ENA where marine stratocumulus clouds can produce drizzle for hours at a time, events observed at SGP often have sudden increases in rain rate that can quickly lead to strong wet radome attenuation, which would lead to much lower KAZR reflectivity values. Three example cases at ENA, NSA, and SGP are shown in Figure 17 to highlight the differences between each site. The offsets between the KAZR and the disdrometer at ENA and NSA are relatively small compared to at SGP. For the SGP case, the first few points between the KAZR and VDIS are similar but then the KAZR reflectivity drops considerably as the rain rate jumps.

Another drawback of the disdrometer comparison at SGP is that the slower sampling frequency of the disdrometer leads to less comparison points available in these events that may not last as long. The disdrometer comparison was also performed with the LD collocated at the Central Facility E13 site, which was operational for a subset of the time period (2020-September 2023), and similar results were observed with increased variability and few comparison points identified. To avoid comparisons at the surface, we will use a different methodology to evaluate the KAZR calibration involving comparisons with the nearest WSR-88D in ice clouds aloft (Section 2.4.3).

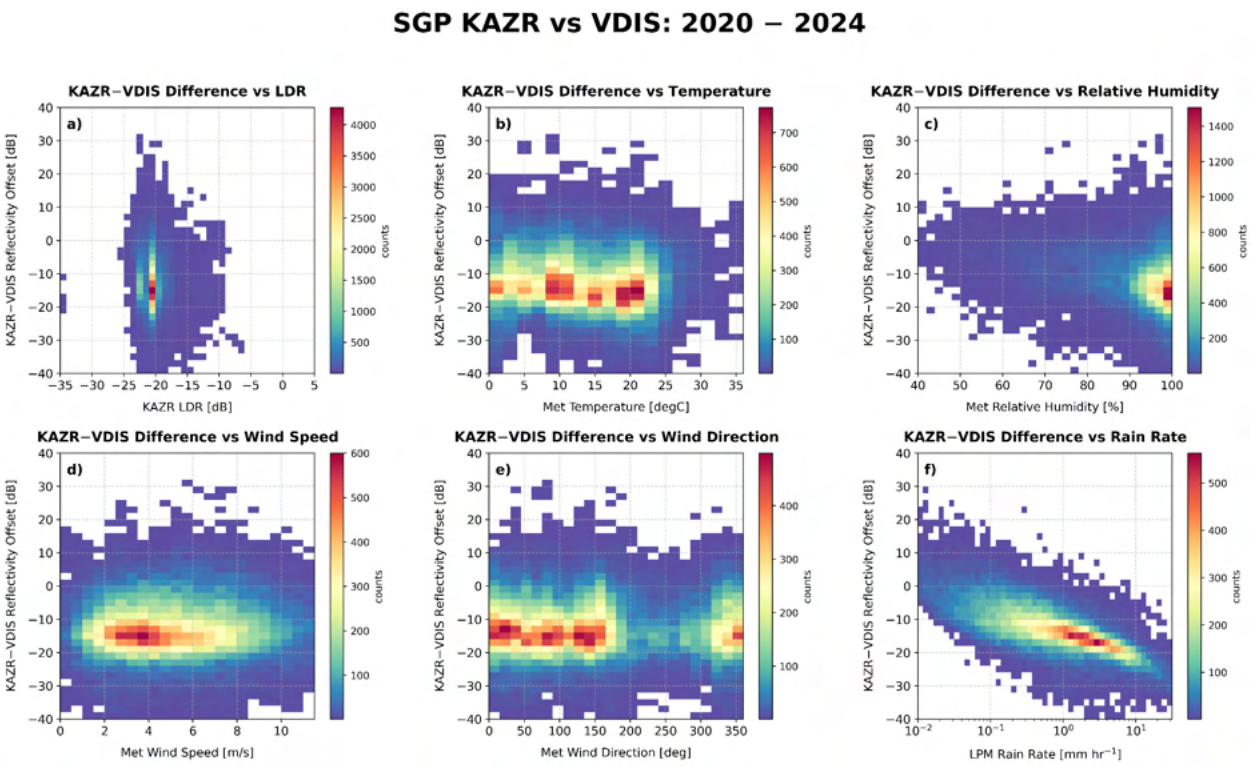

Figure 15. As in Figure 9 but for the SGP KAZR GE mode and the VDIS.

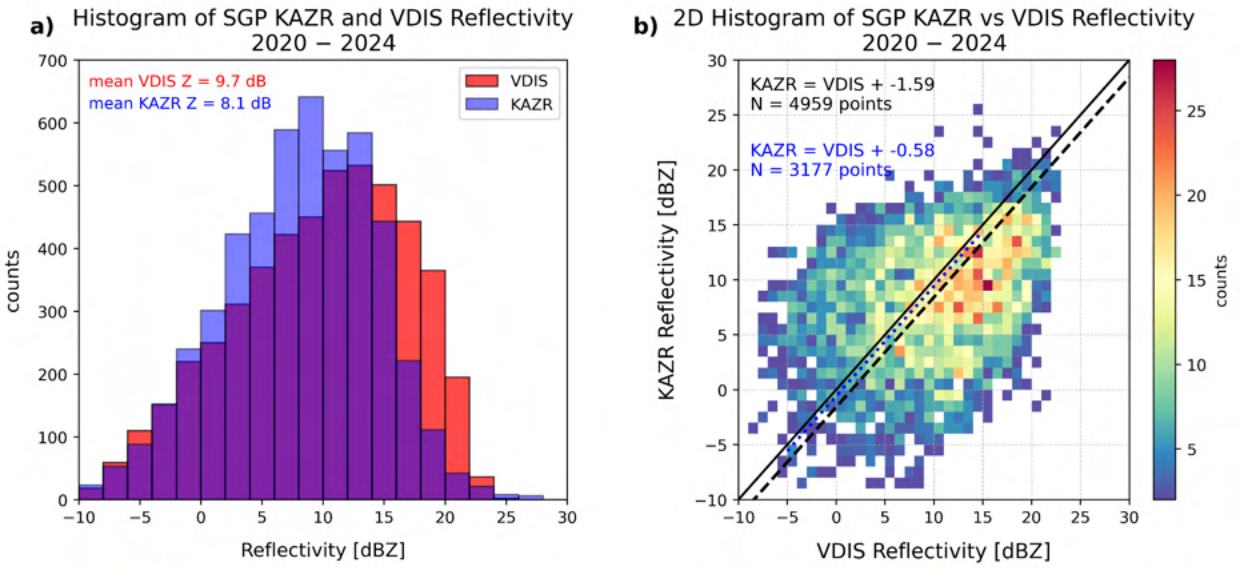

Figure 16. As in Figure 10 but for the SGP KAZR GE mode and the VDIS. The mean offset between KAZR and VDIS when points are between -5 and 15 dBZ is -0.6 dB. The correlation between KAZR and VDIS reflectivity is 0.37.

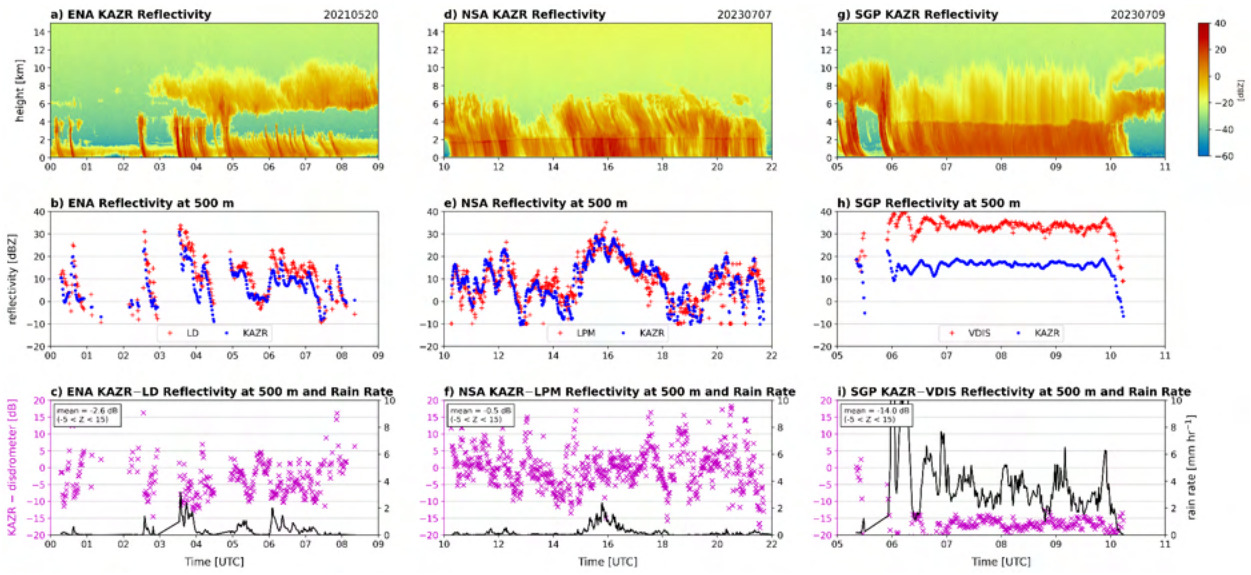

Figure 17. Top panels: Time-height plots of KAZR reflectivity for a) ENA on 20 May 2021 00-09 UTC, d) NSA on 7 July 2023 10-22 UTC, and g) SGP on 9 July 2023 05-11 UTC. Middle panels: Time series of KAZR reflectivity (blue; dBZ) and disdrometer reflectivity (red; dBZ) at 500 m for each case. Bottom panels: Time series of KAZR-disdrometer reflectivity difference (magenta; dB) and disdrometer rain rate (black; mm hr^{-1}). The mean difference for points between -5 and 15 dBZ is shown in the upper left for each case.

2.4 Additional Calibration Methodologies

Additional methodologies are developed for each site to gain more robust results and evaluate some of the uncertainties. Results from each of the methodologies are detailed below.

2.4.1 ENA KAZR versus Disdrometer Following Kollias et al. 2019

Kollias et al. 2019 performed long-term reflectivity comparisons with KAZRs at different sites and CloudSat's W-band cloud profiling radar (CPR). Given the few samples of non-precipitating ice clouds over the ENA site, they performed an additional comparison using the ground-based laser disdrometer. Here, we recreate their methodology using comparisons with both the LD and VDIS from 2020 through 2024.

This methodology is similar to the one detailed above in Section 2.3. KAZR data at 500 m is matched in time with the nearest disdrometer sample and is averaged two minutes before and after. Comparisons are limited to when the reflectivity was between 0 and 20 dBZ and hydrometeor attenuation is estimated using the relationship $A_h = 0.28RR$ (Matrosov 2005), where A_h is the one-way attenuation (dB km^{-1}) and RR is the rain rate from the disdrometer in mm hr^{-1}. The differences are then computed and a 90-day running mean is calculated.

Figure 18 shows the results of this comparison. While the daily differences vary, the 90-day average difference is typically less than 2 dB. The mean of the 90-day average difference with KAZR and the LD (VDIS) is -2.2 (-1.1) dB. An increase in the running mean is observed in the second half of 2023 for the LD comparison, which lines up with when the LD started to have data quality issues. This trend also

agrees well with the analysis in Section 2.3.1. Similar to the previous method using several different thresholds for comparison, these results suggest the ENA KAZR2 is stable during this period with a small bias less than 1-2 dB.

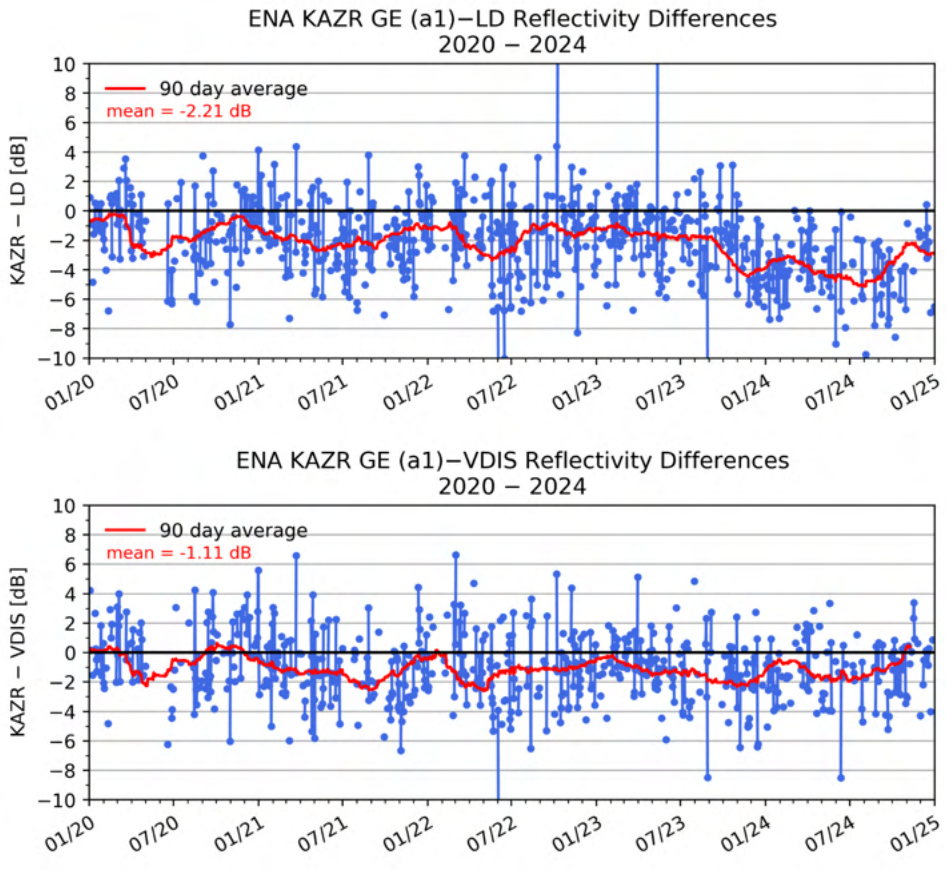

Figure 18. (top) Time series of daily differences between ENA KAZR GE and LD reflectivity (blue) with a 90-day running average applied (red). The mean of the 90-day running average for the calibration time period is -2.2 dB. (bottom) Same as the top but the comparison is with the VDIS reflectivity and the mean of the 90-day running average is -1.1 dB.

2.4.2 NSA KAZR Self-Calibration

There have been a few independent studies of the NSA KAZR calibration in the past, including comparisons with CloudSat's CPR (Kollias et al. 2019) and analysis of liquid water path (LWP; Maahn et al. 2019). Both studies looked at the 2016 season and found the NSA KAZR reflectivity offset was stable around 1-3 dB. While there is currently no calibrated CPR data available to the public for our time frame of interest (as of summer 2025), we can test another more qualitative calibration method used by Matrosov et al. 2022 and the ARM radar team for evaluating KAZR data from the Multidisciplinary Drifting Observatory for the Study of Arctic Climate (MOSAiC) campaign (Matthews et al. 2023). The premise of this methodology is that arctic clouds aloft (above ~ 4 km) in the winter likely have similar statistics from year to year. Thus, average reflectivity values can be calculated from clouds 4 km above ground level at various thresholds and compared with "reference" values from a known calibration period (i.e., 2016). Figure 19 shows the results of these comparisons for each year from 2016 to 2024 for

November through February. The 2021-2024 lines are adjusted for a different calibration constant compared to 2016. The majority of the lines overlap with the 2016 reference line at some reflectivity threshold, suggesting the offset is consistent in time in the winter months. The number of points used for each year for the winter months indicates there is some variability between years (not shown), but it is not clear how much that impacts the results. The number of points between years varies more in November compared to January, which may explain the increased variability in Figure 19 in November. One line stands out, however: November 2024 is significantly lower than the 2016 reference (and other years). This drop in reflectivity occurred from 13 November through 3 December 2024 before the engineer restarted the system and has been documented. This issue also impacted the cross-polar reflectivity and thus the LDR and appeared to be related to the RDS and/or the MCC. Further analysis suggests both GE and MD co-polar reflectivity dropped about 16 dB during this period.

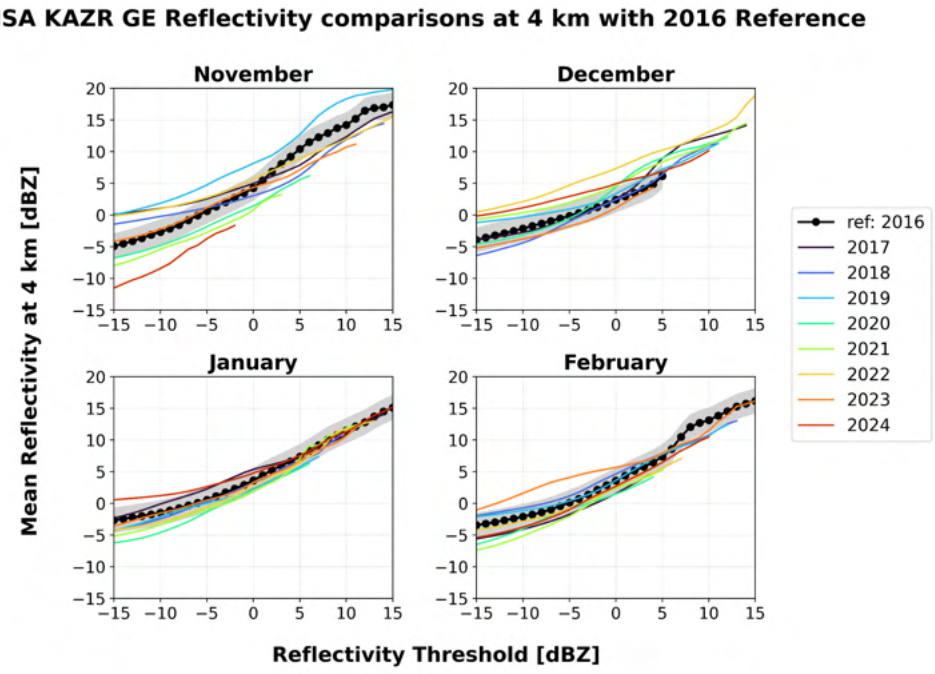

Figure 19. Mean NSA KAZR GE-mode reflectivity at 4 km calculated at thresholds between -15 and 15 dBZ for November through February. Each colored line represents a different year while the dotted black line is the reference year (2016). A 2 dB standard deviation is shown in the shaded grey around the 2016 reference line.

2.4.3 SGP KAZR versus KVNX

The KVNX WSR-88D located near Vance AFB in Oklahoma is an S-band radar that is part of the Next-Generation Weather Radar (NEXRAD) system operated by the National Weather Service. KVNX is the nearest NEXRAD site to SGP and is located about 60 km west of SGP. Here, KVNX is compared with the KAZR to determine any reflectivity offsets.

The columnsect utility in the Python ARM Radar Toolkit (Py-ART; Helmus and Collis 2016) is used to extract profiles from the KVNX plan position indicators (PPIs) over KAZR. These points are compared with the nearest-in-time profiles over KAZR. Given the KVNX beam width and distance from SGP, KAZR profiles are averaged 500 m above and below the nearest range bin to ensure each radar is

sampling roughly the same volume. Several additional thresholds are included to make the comparison as fair as possible. Comparisons are performed in non-precipitating ice clouds aloft to eliminate any impacts on attenuation. Data from soundings shows the melting level fluctuates seasonally but never reaches 6 km. Differential reflectivity (ZDR) and LDR thresholds are also included to ensure small ice crystals are compared, and a reflectivity threshold between -5 and 15 dBZ is used to ensure Rayleigh scattering.

Figure 20 shows the 2D histogram of KAZR GE reflectivity vs KVNX reflectivity in non-precipitating ice profiles. The best fit line through the distribution indicates KAZR is about 1.6 dB less than KVNX when reflectivity is between -5 and 15 dBZ. Daily means of the differences are also calculated to evaluate the trend of the offset. The time series in Figure 21 indicates the offset is fairly consistent through the calibration period, although there is about a 1 dB shift in the offset in early August 2023, likely corresponding to the shift in the radar constant. Before 6 August 2023 the mean offset is -0.9 dB while afterwards the offset is -1.9 dB. Similarly, once the 2D histogram analysis is split at August 2023, there is about a 1 dB difference in the means during each time period (not shown).

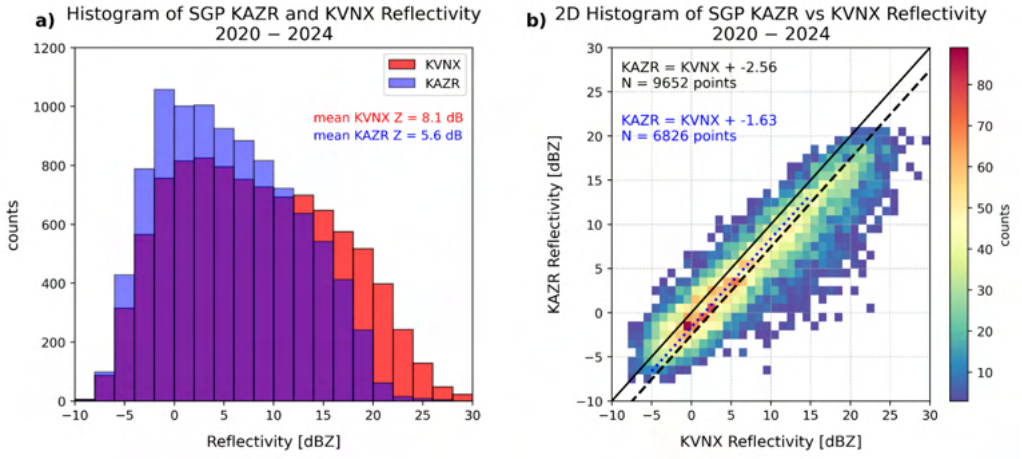

Figure 20. As in Figure 10 but for SGP KAZR GE mode and KVNX. The mean offset between KAZR and KVNX when points are between -5 and 15 dBZ is -1.6 dB. The correlation between KAZR and KVNX reflectivity is 0.85.

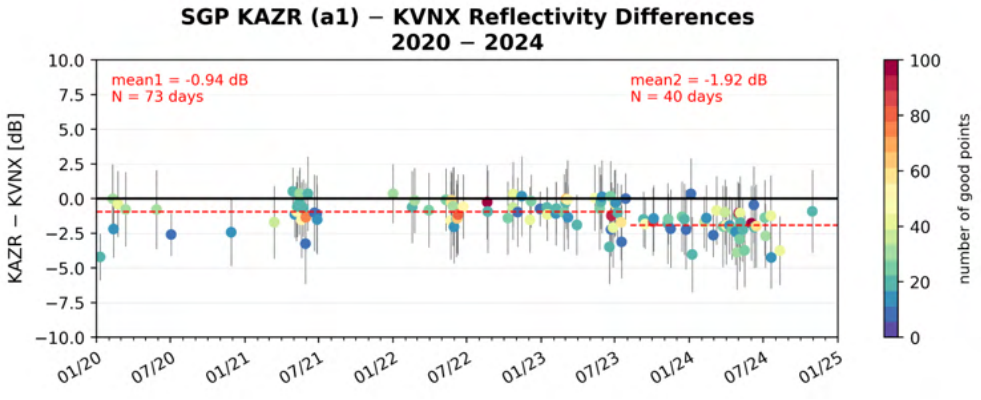

Figure 21. As in Figure 11 but for SGP KAZR GE mode and KVNX. The mean of the daily mean differences before August 2023 is -0.9 dB and 73 days of data were used. The mean after July 2023 is -1.9 dB and 40 additional days were analyzed.

2.5 Summary of KAZR Offsets

A summary of the KAZR reflectivity offsets for each mode at each site is provided below, with final numbers and time periods shown in Table 3.

From the analyses with the LD, we conclude that the ENA KAZR2 GE mode is consistently about 0.5 dB lower than it should be. Based on the GE- versus MD-mode comparison in Section 2.2, the MD mode is 1.2 dB too low from 1 January 2020 until 18 June 2020. The MD mode is then 0.2 dB too low until 25 May 2023 and 2.0 dB too high after 25 May 2023. The PR-mode offset is a function of the transmit power decline and five time periods with varying initial offsets are determined all with a constant slope of 0.003 dB day^{-1}. The initial offset in January 2020 is 7.7 dB, which then increases from there.

At NSA, the KAZR GE mode is about 4.1 dB lower than the disdrometer in the summer of 2021. After the radar constant changes in October 2021, the KAZR agrees much closer with the disdrometer during the summer months of 2022-2024. A qualitative analysis during the winter months that accounts for changes in the radar constant showed similar agreement among the past years except for in November 2024 when the reflectivity dropped around 16 dB. For the GE mode, 4.1 dB is added from January 2020 through 25 October 2021. 0.7 dB is added from 26 October 2021 until 8 May 2024 and 1 July 2024 through 13 November 2024. In May-June 2024, the GE-mode reflectivity needs 3.4 dB added, in mid-November 2024 an additional 16.7 dB is added, and starting 3 December 2024 another 1.0 dB added. The MD mode offsets are mostly consistent across the period, with 1.9 dB added before 26 October 2021 and 1.6 dB added afterwards except in mid-November 2024 when an additional 17.6 dB is needed.

For SGP, given the higher number of samples, less variability, and less uncertainty associated with the KVNX method compared to the disdrometer method, the final offset applied to the SGP KAZR GE data is 1.3 dB before 6 August 2023 and 2.3 dB after 6 August 2023. The comparison between GE and MD mode showed MD was consistently about 0.3-0.5 dB too low, so 1.8 dB is added to the MD mode from 1 January 2020 to 4 November 2020, 1.6 dB between 4 November 2020 and 6 August 2023, and 2.6 dB from 6 August 2023 onwards.

Table 3. Reflectivity offsets (dB) applied to the b1 data during the indicated time frame for each KAZR mode. For the ENA PR mode, *t* represents the number of days since the indicated date.

Site, Mode	Time Frame	Offset Applied (dB)
ENA, GE	20200101-20250101	+0.5
ENA, MD	20200101-20200619	+1.2
	20200619-20230525	+0.2
	20230525-20250101	-2.0
ENA, PR	20200101-20200618	$0.003t + 7.7$ *t = days since 20200101*
	20200618-20220406	$0.003t + 10.0$ *t = days since 20200618*

Site, Mode	Time Frame	Offset Applied (dB)
	20220406-20220506	$0.003t + 8.9$ *t = days since 20220406*
	20220506-20221025	$0.003t + 11.5$ *t = days since 20220406*
	20221025-20250101	$0.003t + 12.5$ *t = days since 20221025*
NSA, GE	20200101-20211026	+4.1
	20211026-20240508	+0.7
	20240508-20240701	+3.4
	20240701-20241113	+0.7
	20241113-20241203	+16.7
	20241203-20250101	+0.7
NSA, MD	20200101-20211026	+1.9
	20211026-20241113	+1.6
	20241113-20241203	+17.6
	20241203-20250101	+0.4
SGP, GE	20200101-20230806	+1.3
	20230806-20250101	+2.3
SGP, MD	20200101-20201104	+1.8
	20201104-20230806	+1.6
	20230806-20250101	+2.6

3.0 Masks

Two masks are developed for the KAZRs. The first is the censor mask which uses the standard deviation of mean Doppler velocity (velocity texture) to distinguish between signal and background noise. The velocity texture threshold used to identify signal from noise is 1.5 m s^{-1} for each KAZR at the fixed sites. An example of the velocity texture and censor mask applied to the NSA KAZR GE and MD modes on 30 July 2024 is shown in Figure 22. The censor mask clearly shows several cloud layers during this day.

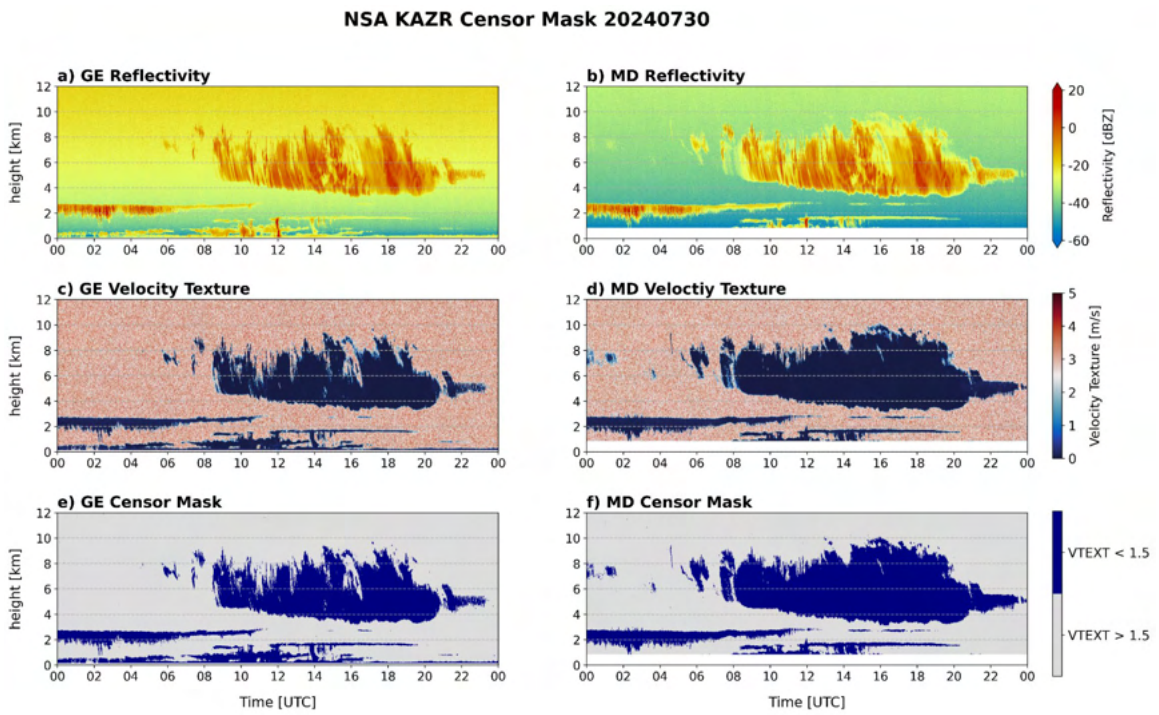

Figure 22. Time-height plots on 30 July 2024 of NSA KAZR a-b) reflectivity (dBZ), c-d) velocity texture (m s^{-1}) and e-f) censor mask (velocity texture > 1.5 m s^{-1} = light grey; < 1.5 m s^{-1} = navy blue) for GE mode (left) and MD mode (right).

The second mask identifies other non-meteorological signals such as clutter, range sidelobes, and insects, which can be prevalent in the KAZR data depending on the site and time of year. Key variables used for each category of the mask are shown in Table 4. The background noise mask is the same as the censor mask and is applied to each mode of the KAZR. Next, ground clutter is identified using reflectivity, velocity, and spectral width. The ground clutter is stationary in time and thus has near-zero velocity and spectral width. Typically, ground clutter is only observed in the GE mode since the first range gate of the MD mode is usually above the ground clutter level. The ground clutter signal is observed daily at ENA (Figure 23).

Table 4. Mask categories, the KAZR modes that the mask is applied to, and key parameters used in the mask.

Mask Category	KAZR Mode	Key Variables
Background Noise	GE, MD, PR	velocity texture
Ground Clutter	GE, MD	reflectivity, velocity, spectral width
Range Sidelobe	MD	SNR, spectral width
Biota	GE, MD	SNR, LDR, LDR texture, reflectivity texture, spectral width

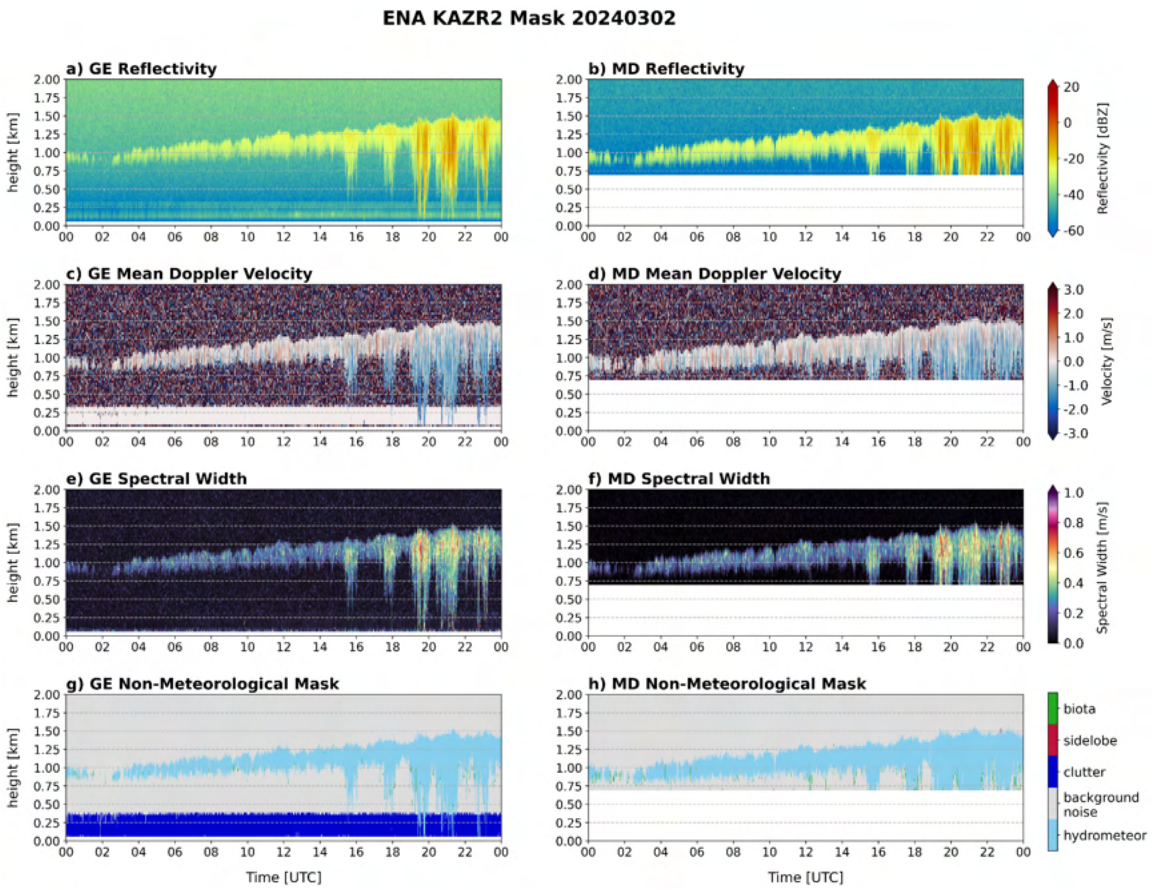

Figure 23. Time-height plots on 2 March 2024 of ENA KAZR2 a-b) reflectivity (dBZ), c-d) mean Doppler velocity (m s^{-1}), e-f) spectral width (m s^{-1}) and g-h) non-meteorological mask (hydrometeor = light blue; background noise = light grey; clutter = blue; sidelobe = red; biota = green) for GE mode (left) and MD mode (right).

Range sidelobes can be found in the MD-mode data especially with strong clouds or precipitation. These sidelobes present as false echoes above cloud top in the MD mode and are a result of the pulse compression. However, the GE mode can be used to estimate the true cloud top height and variables such as SNR and spectral width can be used to identify these false echoes and mask them out. Some details on the methodology for sidelobe detection can be found in Silber et al. (2018). Several additional parameters in the sidelobe detection mask are tuned to optimize the retrieval at each site. Sidelobes are particularly prevalent at NSA, which experiences frequent boundary-layer clouds. Figure 24 shows an example of the non-meteorological mask applied to NSA KAZR data.

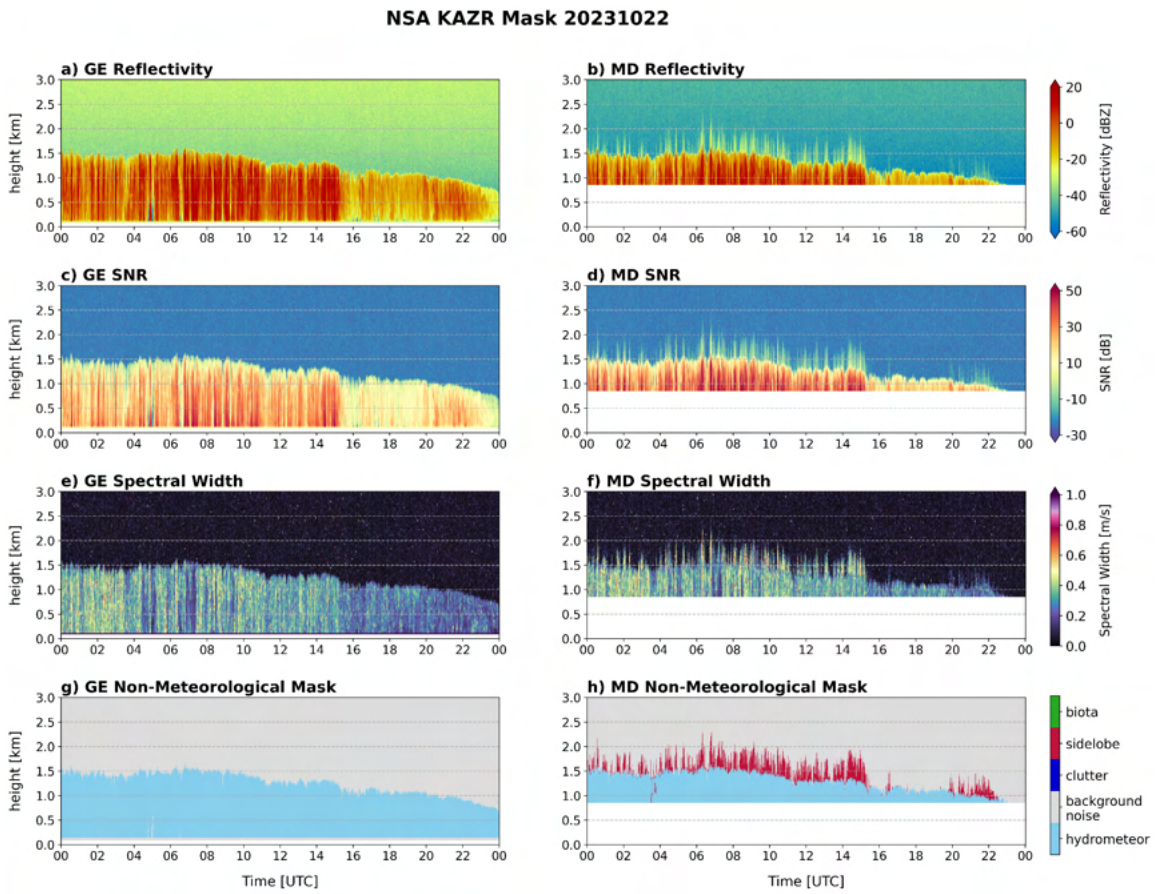

Figure 24. Time-height plots on 22 October 2023 of NSA KAZR a-b) reflectivity (dBZ), c-d) signal-to-noise ratio (dB), e-f) spectral width (m s^{-1}) and g-h) non-meteorological mask (hydrometeor = light blue; background noise = light grey; clutter = blue; sidelobe = red; biota = green) for GE mode (left) and MD mode (right).

The final part of the non-meteorological mask is the biota or insect detection. One of the key radar variables used to distinguish between hydrometeors and biota is the LDR. The LDR for insects is typically higher (> -10 dB) than the LDR for hydrometeors (typically < -15 dB), but the exact values can vary by location. Additionally, there is some overlap between biota and hydrometeor signals, and features like cloud edges and the bright band often have higher LDR. Therefore, a more complex combination of variables is needed to classify the signals appropriately. The resulting biota mask varies for each site both in what variables are used and the thresholds applied for each variable. The biota mask captures the main cloud and biota features fairly well, even at SGP where insects are observed almost daily in the boundary layer. An example of the mask applied to SGP is shown in Figure 25. The biota mask is not computed at NSA given the lack of insects observed.

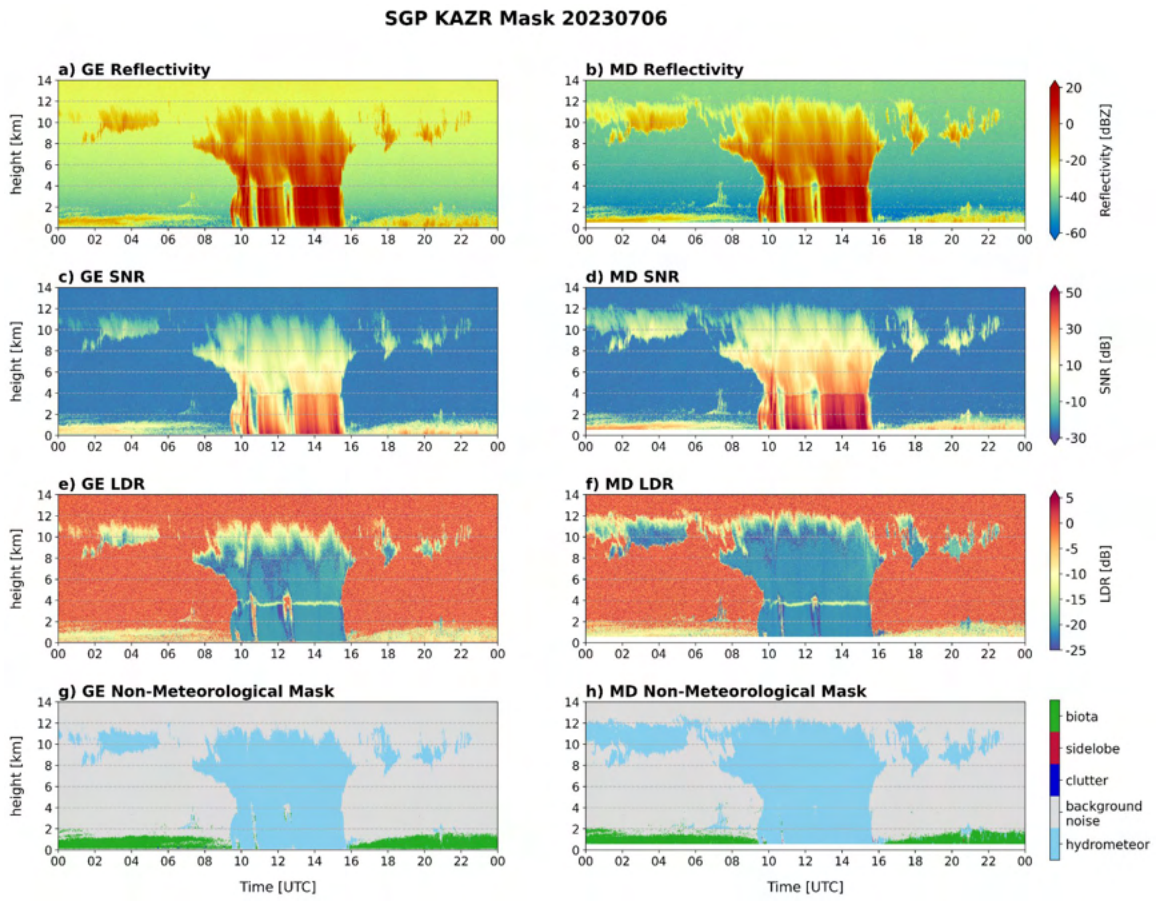

Figure 25. Time-height plots on 6 July 2023 of SGP KAZR a-b) reflectivity (dBZ), c-d) signal-to-noise ratio (dB), e-f) linear depolarization ratio (dB) and g-h) non-meteorological mask (hydrometeor = light blue; background noise = light grey; clutter = blue; sidelobe = red; biota = green) for GE mode (left) and MD mode (right).

4.0 Description of Data Files

Key
Only in KAZR
Only in KAZR2
New variable calculated in b1 data
Correction applied

KAZR File Contents (enakazr2cfrgeqcC1.b1, enakazr2cfrmdqcC1.b1, and enakazr2cfrprqcC1.b1) (nsakazrcfrgeqcC1.b1 and nsakazrcfrmdqcC1.b1) (sgpkazrcfrgeqcC1.b1 and sgpkazrcfrmdqcC1.b1)	
Moments	
co_to_crosspol_correlation_coeff	co-polar to cross-polar correlation coefficient (also known at rhoxh)
linear_depolarization_ratio	linear depolarization ratio, channel unspecified
mean_doppler_velocity	radial mean Doppler velocity, positive for motion away from the instrument
mean_doppler_velocity_crosspolar_v	Doppler velocity, cross-polar for vertical channel
reflectivity	equivalent reflectivity factor with offset applied
reflectivity_crosspolar_v	equivalent reflectivity factor, cross-polar for vertical channel
signal_to_noise_ratio_copolar_h	Signal-to-noise ratio, horizontal channel
signal_to_noise_ratio_crosspolar_v	Signal-to-noise ratio, cross-polar for vertical channel
spectral_width	spectral width
spectral_width_crosspolar_v	spectral width, cross-polar for vertical channel
Masks	
censor_mask	Bit mask 0: no mask 4: velocity_texture_above_threshold
classification_mask	Non-meteorological echo classification mask 0: hydrometeor 1: background noise 2: ground clutter 3: sidelobe 4: biota

5.0 References

Hardin, J, SE. Giangrande, and A Zhou. 2020. Laser Disdrometer Quantities (LDQUANTS) and Video Disdrometer Quantities (VDISQUANTS) Value-Added Products Report. U.S. Department of Energy, Atmospheric Radiation Measurement user facility, Richland, Washington. DOE/SC-ARM-TR-221, https://doi.org/10.2172/1808573

Helmus, JJ and SM Collis. 2016. "The Python ARM Radar Toolkit (Py-ART), a Library for Working with Weather Radar Data in the Python Programming Language." *Journal of Open Research Software* 4(1): e25, http://doi.org/10.5334/jors.119

Kollias, P, B Puigdomènech Treserras, and A Protat. 2019. "Calibration of the 2007-2017 record of Atmospheric Radiation Measurement cloud radar observations using CloudSat." *Atmospheric Measurement Techniques* 12: 4949–4964, https://doi.org/10.5194/amt-12-4949-2019

Matrosov, SY. 2005. "Attenuation-based estimates of rainfall rates aloft with vertically pointing Ka-band radars." *Journal of Atmospheric and Oceanic Technology* 22: 43–54, https://doi.org/10.1175/JTECH-1677.1

Matthews, A, K Johnson, E Schuman, Y-C Feng, S Matrosov, J Comstock, and SE Giangrande. 2023. MOSAiC Radar b1 Processing: Corrections, Calibrations, and Processing Report. U.S. Department of Energy, Atmospheric Radiation Measurement user facility, Richland, Washington. DOE/SC-ARM-TR-293, https://doi.org/10.2172/2229372

Sekelsky, SM. 2002. "Near-field reflectivity and antenna boresight gain corrections for millimeter-wave atmospheric radars." *Journal of Atmospheric and Oceanic Technology* 19(4): 468–477, https://doi.org/10.1175/1520-0426(2002)019<0468:NFRAAB>2.0.CO;2

Silber, I, J Verlinde, EW Eloranta, and M Cadeddu. 2018. "Antarctic cloud macrophysical, thermodynamic phase, and atmospheric inversion coupling properties at McMurdo Station: I. Principal data processing and climatology." *Journal of Geophysical Research – Atmospheres* 123(11): 6099–6121, https://doi.org/10.1029/2018JD028279

Ulaby, FT, RK Moore, and AK Fung. 1981. *Microwave Remote Sensing, vol. I*. Addison-Wesley Publishing Company, Reading, Massachusetts.

Wang, D, MJ Bartholomew, SE Giangrande, and JC Hardin. 2021. Analysis of Three Types of Collocated Disdrometer Measurements at the ARM Southern Great Plains Observatory. U.S. Department of Energy, Atmospheric Radiation Measurement user facility, Richland, Washington. DOE/SC-ARM-TR-275, https://doi.org/10.2172/1828172.

www.arm.gov

U.S. DEPARTMENT OF
ENERGY

Office of Science